Amyloid-β Protein and Neuroglobin Protein as Biomarkers on Brainstem Following Traumatic Brain Injury in Rats

Wenhe Li
Department of Pathology, The Central Hospital of Wuhan, Tongji Medical College, Huazhong University of Science and Technology

Haijun Zhu
Department of Plastic and Cosmetology, The Central Hospital of Wuhan, Tongji Medical College, Huazhong Uinversity of Science and Technology

Yue Liang
Department of Forensic Medicine, Tongji Medical College, Huazhong Uinversity of Science and Technology

Fang Tong
Department of Forensic Medicine, Tongji Medical College of Huazhong University of Science and Technology

Yiwu Zhou (87247559@qq.com)

Research

Keywords: traumatic brain injury, Aβ, NGB, brainstem, biomarkers, β-APP

Posted Date: July 9th, 2020

DOI: https://doi.org/10.21203/rs.3.rs-40711/v1

Abstract

Background: Biomarkers play an important role in accurate diagnosis of traumatic brain injury (TBI). Due to the complexity and diversity of TBI, it is likely that a single biomarker will not be used for exactly diagnose. Amyloid-beta (Aβ) protein is generated by sequential cleavage of amyloid precursor protein (APP) by β- and γ-secretase, which may exert its toxic effects by increasing reactive oxygen species and neuroinflammation in the brain as damage factor of TBI. Its use in diagnosis for TBI is becoming more widespread. Neuroglobin (NGB) protein is great potential to diminish neuronal damage. Most epidemiological evidence suggested that Aβ and NGB may be used as biomarkers on brainstem (BS) following TBI. The aim of this study was to investigate the trend of Aβ and NGB on BS of rats with TBI and to analyze comprehensively them as potential biomarkers.

Methods: Adult male Sprague-Dawley rats were subjected to the modified weight-drop model of closed TBI. Biologic behavior observation, histopathological assessments and western blot assay were performed. Aβ and NGB expression indicated temporal changes in BS after TBI. Their accuracy and efficiency of performing these tasks were calculated and statistical comparisons performed.

Results: The results of Aβ enable us to speculate that the time points of 3 h, 6 h and 12 h may be crucial points for the diagnosis of TBI. NGB expression in the injured had obvious difference versus the control, the points of 1 h and 3 h were apparently higher than the control, and the groups of 12 h and 48 h were two peaks in the present study. Furthermore, the immunofluorescence assay results supported that Aβ and NGB co-localization in the neuros of BS, and the NGB specific expression in the BS of neurons.

Conclusions: Therefore, the expression and change rules of Aβ and NBG in the BS may provide an important foundation for the diagnosis of TBI, damage assessment and therapeutic intervention.

Background

TBI is defined as an alteration in brain function, or other evidence of brain pathology, and caused by an external cause, which is a worldwide public health problem that can result in long-lasting disability [1]. It is often a diagnostic and therapeutic challenge in clinical medicine. The overall annual incidence of TBI in the United States is 506.4 per 100 000 population, the incidence rate of TBI per 100 000 population is 403, 85, and 18 per 100 000 for emergency department (ED) visits, acute hospital discharges and deaths [2]. TBI may occurs when brain physiology and structure are either focally or diffusely disrupted following high-impact contact between the skull and another object, which have high incidence and serious long-term complications [3, 4]. Some of the leading causes of TBI include blunt injury, high falling injury, falling injury and traffic accident, among which traffic accidents was the most common cause [5]. Primary and secondary brain injury are ways to classify the injury processes that occur in brain injury, primary injuries following TBI are deformation of the brain tissue and disruption of normal brain function caused by the external mechanical forces, such as acceleration and deceleration linear forces, rotational forces, forces generated by blast winds associated with blast injury[6]. Secondary brain injury mechanisms include

blood-brain barrier (BBB) breakdown, the release of inflammatory factors, intracellular calcium overload, and reactive oxygen and nitrogen free radical generation [7, 8]. These secondary injury events are considered to account for the development of neurological deficits observed after TBI, including the damage of vascular, neuronal, axonal and glial cell due to the increases of neuro-inflammatory microglia cells, levels of inflammatory cytokines and edema [9, 10]. So far, the application of biomarkers to diagnose TBI and clinical research have progressed rapidly, the neurochemical events generate a host of beneficial and detrimental molecules such as interleukin (IL)-1β, tumor necrosis factor-α (TNF α), and interferon-γ (IFN γ) and oxidative metabolites (nitric oxide, reactive oxygen and nitrogen species), excessive accumulation and deposition of Aβ, apolipoprotein E (Apo E), glial fibrillary acidic protein (GFAP), vimentin (Vim) and NGB [11–15].

Aβ resulting from massive accumulation of amyloid precursor protein (APP) in damaged axons, have been found deposited throughout the brain in about 30% of fatal TBI [16]. It is considered to be via transmembrane cleavage of APP by β-site APP-cleaving enzyme (BACE) and a catalytic component of γ-secretase, presenilin-1 (PS-1)[17]. A number of studies have indicated that Aβ exerts its toxicity in part through activating inflammatory pathways in the brain and promoting the formation of reactive oxygen species (ROS) with a resultant increase in oxidative damage, which are the contribution of Aβ toxicity to oxidative stress in the brain [18]. ROS produce normally for cellular activity and are usually maintained at low physiological levels, while ROS levels exceed the antioxidant capabilities of the cell caused by the abnormal production of Aβ [19, 20]. Thus, Aβ with the result being excessive neuroinflammation and oxidative damage that can disrupt normal cellular functioning and ultimately lead to neuronal death [18]. Previously, Aβ were released into the interstitial fluid, cerebral microdialysis is a preferred sampling method for these biomarkers [21]. The studies revealed that progression of Aβ accumulation was examined in brain tissue with post-TBI survival of up to 3 years, and the temporal dynamics of Aβ amyloid deposition in brain using Pittsburg B-compound (PiB) combined with positron emission tomography (PiB-PET) imaging up to 48 months and Aβ can be measured in both cerebrospinal fluid (CSF) and in blood over time[16, 22, 23]. Epidemiological, pathological and animal studies have documented that Aβ accumulation could be accelerated after TBI and the inhibition of Aβ accumulation in TBI animals improved their cognitive function [24]. Many novel therapeutic approaches have been reported for either cleaning Aβ or diminishing its downstream events [25].

NGB is a vertebrate globin expressed primarily in neurons, bind O_2 and other gaseous messengers, which is induced by hypoxia and ischemia and then play an important role in protecting against brain injury [26, 27]. It is widely expressed in the neurons of vertebrate central and peripheral nervous systems, retina, and endocrine tissues [28]. Apart from its ability to bind oxygen, NGB also functions as an effective free radical scavenger and is neuroprotective within the brain following stroke and TBI [29]. Hypoxia commonly occurs as a secondary injury response to TBI, NGB expression protects neurons from cell death and reactive oxygen species damage [30, 31]. Multiple neuroprotective effects operate by different mechanisms, including inhibit calcium influx, reduce cellular uptake of iron, copper, and zinc, suppress necrosis and apoptosis, and several studies suggest that NGB may positively affect TBI outcomes [32,

33]. The reported results indicated that there was a late, but significant, increase in NGB mRNA expression 7 days post-TBI in WT mice and the subacute increase occurred later that were known to be upregulated at 3 days post-TBI[32].The previous work in the rat and mouse also showed increased NGB expression levels with peak time of 6 hours after TBI[34].

It is of great significance to study the expression of Aβ and NGB in experimental rat BS following TBI and to provide sensitive and specific markers for TBI. Therefore, this present study intends to further explore the BS protein levels of Aβ and NGB at various points using the modified weight-drop model of closed TBI. In the present study, this review article will discuss the evidence from the above study and explore the validity of considered them as biomarkers in the diagnosis and outcome evaluation after TBI in BS.

Materials And Methods

Traumatic brain injury model and experimental procedure

All procedures were approved by the guidelines for the care and use of animals in China. The subjects were eighty male Sprague-Dawley rats obtained from the Animal Experimental Center of Tongji Medical College of Huazhong University of Science and Technology. Adult male Sprague-Dawley rats weighing about 260-300g were used in the experiment. Animals were kept under a 12-h light/dark cycle and allowed free access to food and water. Experimental TBI was performed using a modified weight-drop device previously developed in our laboratory[35-37]. Briefly, a cylindrical steel weight of 450 g was allowed to fall through the tube at a designated height of 2 m to impact the disk. The scalp was sterilized and sutured when their respiratory condition was regular, and the rats were randomized at the desired time points at 1, 3, 6, 12, 24, 48 and 72 h after TBI (n = 8 for each time point). In the sham group, rats underwent the surgical procedure without impact.

Tissue preparation and histopathological assessments

On the basis of previously described concerning the brain tissue preparation, the rats recovered and were observed for 1 - 72 hours, after which they were euthanized using a lethal dose of sodium pentobarbital given IP [35, 38, 39]. In short, the animals were perfused with heparinized saline to remove blood from the intravascular compartment, followed by perfusion-fixation with 4% paraformaldehyde. The brain was harvested and photographed to document surface hemorrhages. The BS was then divided equally by a sagittal cut to include the basal interpeduncular regions of the brain, pons, and pyramids. One part of the brain was processed and embedded in paraffin for histopathological examination. Tissue sections (4 μm thickness) were prepared for hematoxylin and eosin (HE), Luxol-fast blue (LFB), immunohistochemistry (IHC) and immunofluorescence analyses. Rat BS sections were stained with HE and LFB as described previously [40-43]. The other half was quickly dropped in liquid nitrogen for western blot analysis.

Immunohistochemistry

The procedure of IHC was based on the previous study [35, 44]. IHC analysis was performed on paraffin-embedded 4 μm BS sections. After de-paraffinization, the slides were washed three times with distilled water and incubated for 20 min in citrate buffer (pH 6.0) for antigen retrieval using microwave oven, and then blocked for endogenous peroxides with 3% hydrogen peroxide. After the citrate buffer cooled to room temperature and washed three times with phosphate buffered saline (PBS, pH 7.4). The sections were incubated with rabbit monoclonal anti-β-APP antibody (ab32136, 1:2000, Abcam, American), polyclonal rabbit anti-Aβ antibody (ab2539, 1:2000, Abcam, American) and monoclonal mice anti-NGB antibody (ab37258, 1:400, Abcam, American) overnight at 4℃. The following day, the sections were washed three times in PBS for 10 min each, followed by the incubation with ready-to-use SABC (rabbit IgG) kit (Google Biological Technology, Wuhan, China) for 1 h at room temperature Thereafter, the sections were washed three times in PBS for 5 min each. The immunostaining was visualized with 3, 3'-diaminobenzidine (DAB) for brown color development, and sections were counterstained with hematoxylin (Google Biological Technology, Wuhan, China). Final three PBS washes were performed for 5 min each. The sections were allowed to dry and dipped for 5 min each in 75–90–95–95–100–100 % ethanol solutions, followed by two treatments for 10 min each in xylene. Finally, the sections were cover slipped. For control experiments, primary antibodies were omitted. The slides were scanned and examined under Nikon Eclipse 90i microscope (Tokyo, Japan) system using 20 x objective. As for the quantitative analyses of immunohistochemistry, the number of Aβ and NGB immunopositivity staining were counted in the BS using ImageJ software. The image analysis was performed with the default parameter setting, and visual inspection of markup images was performed to confirm that the algorithm results were sufficiently accurate for the purpose of specific biomarker quantification. The positivity value was expressed as a ratio of positive pixels detected (brown staining) to total area. Analysis was performed at full 200 x magnification.

Western blot analysis

The protein expression of Aβ and NGB were examined by western blot analysis. Rats were killed, and the brain tissues were separated. The protein was extracted with RIPA Lysis Buffer (Beyotime, Haimen, China) according to the manufacturer's instructions. Protein concentrations were quantified using a BCA Protein Assay Kit (Beyotime, Haimen, China). Equal amounts of protein samples (20μg) were subjected to 10% SDS-PAGE separation and transferred onto polyvinylidene difluoride membranes. The blots were blocked with 5% fat-free milk in TBS mixed with 0.1% Tween and then incubated overnight at 4 °C with specific antibodies against Aβ (1:1000, Abcam, Cambridge, UK, USA) and NGB (1:1000, Abcam, Cambridge, UK, USA). After three washes with TBST, the membranes were incubated with the corresponding secondary antibodies for 1h at room temperature. The protein bands were visualized using enhanced chemiluminescence kit (Thermo, USA) according to the manufacturer's instructions. β-actin was used as an internal control.

Immunofluorescence assay

We detected the distribution of Aβ and NGB using an immunofluorescence method. Rats were anesthetized and transcardially perfused with saline followed by 4% paraformaldehyde. Brains were removed, post-fixed and dehydrated in graded ethanol solutions. We blocked the nonspecific binding with donkey serum albumin following antigen retrieval. Then the sections were incubated in primary antibody overnight at 4 °C (Aβ 1:100 Abcam, Cambridge, UK, USA; NGB 1:100 Abcam, Cambridge, UK, USA). The following day, the sections were washed and incubated with fluorescently tagged secondary antibody. Negative controls were performed in the absence of primary antibody.

Statistical Analysis

All experiments were performed independently at least in triplicate. Statistical analysis was conducted by using GraphPad Prism 5.0. The values were the mean ± S.E.M. Statistical comparisons were analyzed using a one-way analysis of variance (ANOVA) followed by a Fisher post hoc test to correct for multiple comparisons. Values of *P* less than 0.05 were considered to indicate statistical significance.

Results

In the study, the overall mortality rate was 50 %, and the rats died in a short time after TBI if the opisthotonus and apnea continued and still not have autonomous respiration.

The skull fracture and epidural hematoma were not seen in TBI group and control group. There was no obvious cerebral contusion. The control group had no abnormity **(Fig. 1a)**. Additionally, swelling brain tissue, dilatating and congesting vessels, prominent subarachnoid hemorrhage located at the base of brain and BS could be observed in the TBI group (**Fig. 1b**).

Histopathological findings

Upon gross observation, HE, LFB and β-APP staining were used to evaluate the damage of BS. In the control animals, no obvious pathology was observed. BS contusion, interstitial edema, degenerative and necrotic neurons could be seen in the injured groups (**Fig. 2a – 2c**). At 1 h post-injury, the axons were irregular edema and wavy changes (**Fig. 2d**). Mild circuity and inflated terminal of the axons appeared and the retraction balls (RBs) started to form at 3h group (**Fig. 2e**). The number and range of damage axons gradually increased from 6 to 24 h (**Fig. 2f - 2h**). Among these time points, the number of RBs were significantly risen, especially the 24h group. The region of swelling axons and the number of RBs slightly declined from 48 h to 72 h (**Fig. 2i-2j**). Meanwhile, LFB staining showed that nerve myelin was neatly arranged in the sham group (**Fig. 3a**). The distribution of lightly stained nerve myelin was sparse at TBI groups. Swollen, layered, separated and disintegrated nerve myelin appeared at 1 h (**Fig. 3b**). The range of edema and disintegration were further enlarged and the number of clumps caused by the aggregative myelin were increased from 3 h to 6 h (**Fig. 3c**). As for the injured 12 h group, the number of clumps resulted from myelin disintegration and fragmentation was further enlarged (**Fig. 3d**). The diffuse distribution of myelin was disorganized and significant vacuolar degeneration at 24 h point (**Fig. 3e**). The number of myelin fragments was reduced from 48 h – 72 h after injury (**Fig. 3f**). For further verification of

TBI, the BS sections were stained with the anti-β-APP antibody. At the control group, the IHC staining of β-APP was weakly positive (**Fig. 4a**). While in the injured groups, β-APP positive axons were slightly circuitous, swelling and beaded change since 1 h post-TBI (**Fig. 4b**). A few RBs formed at 3 h group (**Fig. 4c**), the number of immunopositivity RBs increased and became more obvious from 3 h - 6 h (**Fig. 4d**). The positive axons were obvious, and the number and range of RBs were further expanded after 12 h post-TBI (**Fig. 4e**). Typical RBs were gradually increased from 24 h - 72 h and reaching the maximum at 72 h (**Fig. 4f - 4h**).

The IHC and western blot analyses of Aβ

In the control group, there were weak positive located in the cytoplasm and small blood vessels (**Fig. 5a**). The positive cytoplasm and small blood vessels of the BS were enlarged at all points after TBI. The immunopositivity started after 1 h post-TBI. The Aβ expression of neurocytes and small vessels were enhanced from 1 h - 72 h (**Fig. 5b - 5h**). The semi-quantitative analysis of Aβ using immunohistochemistry was shown in the table, and the Aβ integrate optical density (IOD) value of the injured groups were higher than the control group. The IOD value at 3 h and 6 h groups were significantly higher than the control. The IOD values of 3 h and 24 h, 3 h and 48 h were statistically significant. The differences between 6 h and 24 h, 6 h and 48 h had significant statistical difference.

The western blot of Aβ was shown and a clear band was visible near 87KDa on the picture (**Fig. 6**). The quantitative analysis indicated that the expression of Aβ began to increase from 1 h to 6 h. Then, there was a small decline from 6 h to 12 h. The second obvious expression subsequently appeared, increasing to 24 h. The second decrease occurred since 24 h post-TBI. The analysis revealed that Aβ expression of all experimental groups were higher than the control group, the 6 h and 24 h groups were extremely significant difference compared with the control group.

The IHC and western blot analyses of NGB

There were weak positive in the control (**Fig. 7a**). The injured BS NGB immunoreactivity abated from 1 h to 6 h post-TBI. Until 12 h post-TBI, the positive NGB enhanced than previously. From 24 h to 48 h, the intensity and intensity of positive BS nerve cells were fewer compared with 12 h group. At 72 h, nerve cells were still positive expression (**Fig. 7b - 7h**). The semi-quantitative analysis of NGB was shown, and the IOD values in the experimental groups were higher compared to the control group in the table. The 1 h and 3 h groups were significantly different from the control group. Additionally, the 3 h group was significantly higher in comparison with 72 h, and they had a significant statistical difference.

The western blot of NGB was revealed near 17KDa on the film (**Fig. 8**). The quantitative analysis shown that the expression of NGB increased remarkably after 1 h post-TBI. Then, the expression of NGB declined gradually from 1 h to 6 h and the minimum value occurred at 6 h point. Subsequently, the second distinct expression appeared, increasing to 12 h. The expression fallen back since 24 h post-TBI. The analysis revealed that the NGB quantities of all experimental groups were higher than the control group.

Immunofluorescence assay

In the immunofluorescent labeling experiments, tissue was double labeled with antibodies against both β - APP and Aβ, Aβ and NGB. Many of the Aβ positive sites showed co-localization with β - APP. The result suggested that β - APP and Aβ were distributed in neurons and axons (**Fig. 9a**). In addition, we observed similar patterns of punctate labeling, but found that areas of more concentrated NGB deposition were localized within Aβ -positive neurons. By contrast, BS tissues exposed to Aβ and NGB antibody failed to show the small blood vessels co-localization of the two markers. The results supported that Aβ and NGB co-localization in the neurons of BS (**Fig. 9b**).

Discussion

In our prior study, the Marmarou model was used to produce TBI in rats [35]. In the present study, a noninvasive modified weight-drop mouse model to produce TBI and the presented weight-drop model used a 2.0 m guided, free-falling weight to produce brain injury. The mortality rates range from 35% – 50%. As previously described, the severity of brain injury can be easily controlled through the adjustment of mass of the weight and the falling height used to produce injury, the falling height determine the mortality rate [45, 46]. Approximately 30–35% of patients admitted with moderate-to-severe TBI die, Australian studies have revealed acute mortality rates of 30% – 35% during the first 6 months after severe TBI, or even 50% mortality of patients caused by TBI has been reported [47, 48]. The ease and rapidity of the modified weight-drop model along with the outcome produced, made it a clinically relevant model of TBI. Neuropathological and imaging studies have emphasized that diffuse cell tissue damage occurs in TBI, and the white matter which is characterized by axonal stretching, disruption, and eventual separation of nerve fiber [49–52]. Previous animal studies regard the BS as the principle site of action of TBI [53]. Additionally, animal autopsy studies have shown that axonal damage are most obvious in BS white matter [54]. Therefore, there appeared to be sufficient experimental and animal evidence indicating that BS may be especially susceptible to the effects of TBI. Considered that the BS may represent an important predilection site in TBI.

In the present study, gross and pathologic examination revealed evident edema, diffuse subarachnoid hemorrhage (SAH) and minimal supratentorial intraparenchymal hemorrhage. And petechial hemorrhages were noted in ventral BS segments and in the cerebellum. Petechial hemorrhage sited in the BS and cerebellum and confined to periventricular regions of the forebrain that found in previous studies of human and experimental TBI model [55, 56]. Microscopic examination of HE and LFB -stained slides indicated pathologic changes of BS in rats with different dependent time. BS contusion, interstitial edema, degenerative and necrotic neurons and RBs could be seen in the injured groups. The obvious RBs formed at 3 h group, and the number and range of injured axons gradually increased to 72 h. In addition, LFB staining shown that swollen, layered, separated and disintegrated nerve myelin induced by TBI at 1 h. The extent and range of clumps caused by the aggregative myelin were increased from 3 h to 24 h, and significant vacuolar degeneration occurred at 12 h point. The white matter structure areas were not stained with LFB, which was assumed to represent loss of myelin and a major pathologic process in TBI,

and this was reflected by decreased LFB staining intensity. Currently, these results were consistent with histological HE and LFB measurements of TBI [44, 57]. To confirm the above results, damaged axons were labeled by β - APP immunohistochemistry, which has been reported to be a very sensitive marker for axonal damage in a number of experimental conditions as well as in pathological studies in humans [58, 59]. This result showed that RBs could be detected in the BS at 3 h, and the extent enhanced with time extending, the time windows and regional distribution for β-APP-positive immunostaining were in accord with previous experimental studies [35].

Previous experimental animal models and human tissue of brain injury have been used employing a number of markers [60–62]. However, very little research has been employed to use for the exact timeframe of BS after TBI in animal model [63]. Because of the complex nature of post-traumatic pathology, temporal changes in biomarkers expression may provide more insight than examination of a single time point. A temporal analysis could provide insight to the progression of TBI or pathology and identify novel targets for diagnoses which would be overlooked with analysis at a single time point. The purpose of our study was to identify potential sensitive biomarkers for the early diagnosis of TBI in humans. Aβ is a hallmark of all AD cases, previous studies found in 30% of postmortem acute TBI cases and 40–45% of chronic traumatic encephalopathy (CTE) cases associated with inconsistent deposits of diffuse, neuritic or vascular plaques [64]. And aggregation and deposition of Aβ is accelerated after an acute TBI event, appearing even in a span of hours [65]. Our data showed that a temporal changes expression of Aβ can be detected in BS of all groups. The expression of Aβ began to increase from 1 h to 6 h after TBI, then a slightly decline appeared between 6 h and 12 h. The expression risen again following a fall, increasing to 24 h. Subsequently, the second fall occurred since 72 h post-TBI. The Aβ expression of 3 h, 6 h and 24 h groups were markedly increased compared with the control. The comparison of 3 h and 24 h, 3 h and 48 h were statistically significant. The expression Aβ in 6 h group was significantly higher than that in 24 h group and 48 h group. These results enable us to speculate that the time points of 3 h, 6 h and 12 h may be crucial points for the diagnosis of TBI.

NGB was a novel discovered globin in 2000, which is an oxygen-binding protein that supplies oxygen to hypoxic tissue [66]. Evidence exists to support that NGB play an important role, which is upregulated after TBI to assist in promoting cell survival [67]. Numerous experimental studies and in the case of TBI indicated that overexpression of NGB effectively counteracted tissue injury [68]. Previously reported study demonstrated that NGB expression with asynchronous time course changes in mild TBI [69]. Some previous results indicated that NGB mRNA expression rapidly increased in the rat cerebral cortex, and peaked at 30 minutes and 48 hours following TBI using real-time PCR, and IHC staining demonstrated that NGB expression increased and remained high 2 hours to 5 days following injury [70]. At the same period, the result reported that the NGB expression level in neurons increased continuously from 2 h after injury, and reached a peak at 16 h after which it decreased sharply [34]. In our study, the results demonstrated that NGB expressed in the injured and control groups by IHC and western blot examinations. A temporal changes expression of NGB was found. The extent of immunoreactivity was enhanced obviously after 1 h post-TBI. Then the expression receded from 1 h to 6 h, the 12 h group positive staining slightly increased than 6 h, the second decline occurred since 24 h. Additionally, the film

analysis indicated that the expression of NGB in the injured had obvious difference versus the control (p 0.05), the groups of 1 h and 3 h were apparently higher than the control, the NGB expression between 3 h and 72 h had a significant difference. The groups of 12 h and 48 h were two peaks in the present study. Thus, we considered that the NGB expression presented a regular change and the results have a great significance for screening the biomarkers in BS following TBI.

Conclusions

In the present study, Aβ and NGB expression indicated temporal changes in BS after TBI. Among these time points, the Aβ expression of 6 h and 24 h had significant difference compared with the other injured groups and the control. Moreover, 1 h and 12 h were also crucial for detecting the expression NGB. We inferred that 1 h, 6 h and 24 h were important time points accompanied by crucial pathophysiological changes from the above results, especially at 1 h post - TBI. Aβ was used in combination with NGB for diagnosing and monitoring TBI in the early stage. They were regarded as biomarkers for the evaluation and prognosis of TBI.

Abbreviations

TBI: Traumatic brain injury; A: Amyloid-beta; APP: Amyloid precursor protein; NGB: Neuroglobin; BS: Brainstem; ED: Emergency department; BBB: Blood-brain barrier; IL: Interleukin; TNF α: Tumor necrosis factor-α; IFN γ: Interferon-γ; Apo E: Apolipoprotein E; GFAP: Glial fibrillary acidic protein; Vim: Vimentin; β-APP:β-site amyloid precursor protein; BACE: β-site APP-cleaving enzyme; PS-1:Presenilin-1; ROS: Reactive oxygen species; PiB: Pittsburg B-compound; PiB-PET: Pittsburg B-compound combined with positron emission tomography; CSF: Cerebrospinal fluid; HE: Hematoxylin and eosin; LFB: Luxol-fast blue; IHC: Immunohistochemistry; ANOVA: One-way analysis of variance; SAH: Subarachnoid hemorrhage; CTE: Chronic traumatic encephalopathy

Declarations

Competing interests

The authors declare that they have no competing interests.

Funding

This work was supported by grant from National Key Research and Development Program of China (No. 2018YFC0807203).

Authors' contributions

WHL performed the experiments and revised the manuscript; HJZ, YL and FT contributed to data analysis and interpretation of the data; YWZ conceived the study, participated in its design, and helped draft and

edit the manuscript. All authors read and approved the final manuscript.

Acknowledgements

We thank all of the staff at the Department of Forensic Medicine, Tongji Medical College of Huazhong University of Science and Technology, who contributed to the completion of this study.

Author details

[1]Department of Forensic Medicine, Tongji Medical College of Huazhong University of Science and Technology, NO.13 Hangkong Road, Wuhan 430030, People's Republic of China

[2]Department of Pathology, The Central Hospital of Wuhan, Tongji Medical College, Huazhong University of Science and Technology, Wuhan, People's Republic of China

[3]Department of Plastic and Cosmetology, The Central Hospital of Wuhan, Tongji Medical College, Huazhong University of Science and Technology, Wuhan, People's Republic of China

References

1. Andelic N. The epidemiology of traumatic brain injury. Journal of Head Trauma Rehabilitation. 2013;12(25):72-80.
2. Faul M, Xu L, Wald MM, Coronado VG. Traumatic brain injury in the United States: Emergency department visits, hospitalizations, and deaths. Emergency Service Hospital. 2010.
3. Witcher KG, Eiferman DS, Godbout JP. Priming the Inflammatory Pump of the CNS after Traumatic Brain Injury. Trends in Neurosciences. 2015;38(10):609-20.
4. Thurman DJ. The Epidemiology of Traumatic Brain Injury in Children and Youths: A Review of Research Since 1990. Journal of Child Neurology. 2016;31(1):20.
5. Faul M, Xu L, Wald MM, Coronado VG. Traumatic brain injury in the United States: emergency department visits, hospitalizations, and deaths. Emergency Service Hospital. 2004;16(Suppliment 1):A268.
6. Mckee AC, Daneshvar DH. The neuropathology of traumatic brain injury. Handbook of Clinical Neurology. 2015;127:45.
7. Stahel PF, Shohami E, Younis FM, Kariya K, Otto VI, Lenzlinger PM, Grosjean MB, Eugster HP, Trentz O, Kossmann T. Experimental Closed Head Injury|[colon]| Analysis of Neurological Outcome, Blood-Brain Barrier Dysfunction, Intracranial Neutrophil Infiltration, and Neuronal Cell Death in Mice Deficient in Genes for Pro-Inflammatory Cytokines. Journal of Cerebral Blood Flow & Metabolism Official Journal of the International Society of Cerebral Blood Flow & Metabolism. 2000;20(2):369-80.
8. Sajja VSSS, Hlavac N, Vandevord PJ. Role of Glia in Memory Deficits Following Traumatic Brain Injury: Biomarkers of Glia Dysfunction. Frontiers in Integrative Neuroscience. 2016;10(129):7.

9. Bingham D, John CM, Levin J, Panter SS, Jarvis GA. Post-injury conditioning with lipopolysaccharide or lipooligosaccharide reduces inflammation in the brain. Journal of Neuroimmunology. 2013;256(1-2):28-37.
10. Songarj P, Luh C, Staib-Lasarzik I, Engelhard K, Moosmann B, Thal SC. The antioxidative, non-psychoactive tricyclic phenothiazine reduces brain damage after experimental traumatic brain injury in mice. Neuroscience Letters. 2015;584(1):253-8.
11. Block ML, Hong JS. Microglia and inflammation-mediated neurodegeneration: multiple triggers with a common mechanism. Progress in Neurobiology. 2005;76(2):77.
12. Golde TE, Dickson D, Hutton M. Filling the gaps in the abeta cascade hypothesis of Alzheimer's disease. Current Alzheimer Research. 2006;3(5):421-30.
13. Zhong J, Cheng C, Liu H, Huang Z, Wu Y, Teng Z, He J, Zhang H, Wu J, Cao F. Bexarotene protects against traumatic brain injury in mice partially through apolipoprotein E. Neuroscience. 2017;343:434.
14. Menet V, Prieto M, Privat A. Axonal Plasticity and Functional Recovery after Spinal Cord Injury in Mice Deficient in Both Glial Fibrillary Acidic Protein and Vimentin Genes. Proceedings of the National Academy of Sciences of the United States of America. 2003;100(15):8999-9004.
15. Jin K, Mao Y, Mao X, Xie L, Greenberg DA. Neuroglobin expression in ischemic stroke. Stroke. 2010;41(3):557-9.
16. Chen XH, Johnson VE, Uryu K, Trojanowski JQ, Smith DH. A lack of amyloid beta plaques despite persistent accumulation of amyloid beta in axons of long-term survivors of traumatic brain injury. Brain Pathology. 2010;19(2):214-23.
17. Chen XH, Siman R, Iwata A, Meaney DF, Trojanowski JQ, Smith DH. Long-term accumulation of amyloid-beta, beta-secretase, presenilin-1, and caspase-3 in damaged axons following brain trauma. American Journal of Pathology. 2004;165(2):357.
18. Nell HJ, Au JL, Giordano CR, Terlecky SR, Walton PA, Whitehead SN, Cechetto DF. Targeted Antioxidant, Catalase-SKL, Reduces Beta-Amyloid Toxicity in the Rat Brain. Brain Pathology. 2016;27(1):86.
19. Markesbery WR, Carney JM. Oxidative Alterations in Alzheimer's Disease. Brain Pathology. 1999;9(1):133-46.
20. Tabner BJ, Elagnaf OM, German MJ, Fullwood NJ, Allsop D. Protein aggregation, metals and oxidative stress in neurodegenerative diseases. Biochemical Society Transactions. 2005;33(5):1082-6.
21. Marklund N, Farrokhnia N, Hånell A, Vanmechelen E, Enblad P, Zetterberg H, Blennow K, Hillered L. Monitoring of β-amyloid dynamics after human traumatic brain injury. Journal of Neurotrauma. 2014;31(1):42-55.
22. Toledo JB, Xie SX, Trojanowski JQ, Shaw LM. Longitudinal change in CSF Tau and Aβ biomarkers for up to 48 months in ADNI. Acta Neuropathologica. 2013;126(5):659-70.

23. Abbasowa L, Heegaard NHH. A systematic review of amyloid-β peptides as putative mediators of the association between affective disorders and Alzheimer□s disease. Journal of Affective Disorders. 2014;168:167-83.
24. Yang ST, Hsiao IT, Hsieh CJ, Chiang YH, Yen TC, Chiu WT, Lin KJ, Hu CJ. Accumulation of amyloid in cognitive impairment after mild traumatic brain injury. Journal of the Neurological Sciences. 2014;349(1-2):99.
25. Mangialasche F, Solomon A, Winblad B, Mecocci P, Kivipelto M. Alzheimer's disease: clinical trials and drug development. Lancet Neurology. 2010;9(7):702.
26. Burmester T, Weich B, Reinhardt S, Hankeln T. A vertebrate globin expressed in brain2000;407(6803):520-3.
27. KhanAA, Mao XO, Banwait S, Jin K, Greenberg DA. Neuroglobin attenuates beta-amyloid neurotoxicity in vitro and transgenic Alzheimer phenotype in vivo. Proceedings of the National Academy of Sciences of the United States of America. 2007;104(48):19114.
28. Zhao S, Yu Z, Zhao G, Xing C, Hayakawa K, Whalen MJ, Lok JM, Lo EH, Wang X. Neuroglobin-overexpression reduces traumatic brain lesion size in mice. Bmc Neuroscience. 2012;13(1):67.
29. Li W, Wu Y, Ren C, Lu Y, Gao Y, Zheng X, Zhang C. The activity of recombinant human neuroglobin as an antioxidant and free radical scavenger. Proteins-structure Function & Bioinformatics. 2011;79(1):115.
30. Anderson J, Sandhir R, Hamilton ES, Berman NEJ. Impaired Expression of Neuroprotective Molecules in the HIF-1α Pathway following Traumatic Brain Injury in Aged Mice. Journal of neurotrauma. 2009;26(9):1557.
31. Khan AA, Mao XO, Banwait S, Dermardirossian CM, Bokoch GM, Jin K, Greenberg DA. Regulation of hypoxic neuronal death signaling by neuroglobin. Faseb Journal. 2008;22(6):1737-47.
32. Taylor JM, Kelley B, Gregory EJ, Berman NE. Neuroglobin overexpression improves sensorimotor outcomes in a mouse model of traumatic brain injury. Neuroscience Letters. 2014;577:125-9.
33. Duong T, Witting P, St, Parry S, Kennerson M, Lai B, Vogt S, Lay P, Harris H. Multiple protective activities of neuroglobin in cultured neuronal cells exposed to hypoxia re-oxygenation injury. Journal of Neurochemistry. 2009;108(5):1143–54.
34. Shang A, Liu K, Wang H, Wang J, Hang X, Yang Y, Wang Z, Zhang C, Zhou D. Neuroprotective effects of neuroglobin after mechanical injury. Neurological Sciences. 2012;33(3):551-8.
35. Li S, Sun Y, Shan D, Feng B, Xing J, Duan Y, Dai J, Lei H, Zhou Y. Temporal profiles of axonal injury following impact acceleration traumatic brain injury in rats--a comparative study with diffusion tensor imaging and morphological analysis. International Journal of Legal Medicine. 2013;127(1):159-67.
36. Marmarou A, Foda MA, Van dBW, Campbell J, Kita H, Demetriadou K. A new model of diffuse brain injury in rats. Part I: Pathophysiology and biomechanics. Journal of Neurosurgery. 1994;80(2):291.
37. Marmarou CR, Walker SA, Davis CL, Povlishock JT. Quantitative analysis of the relationship between intra- axonal neurofilament compaction and impaired axonal transport following diffuse traumatic

brain injury. Journal of Neurotrauma. 2005;22(10):1066.

38. Kilbourne M, Kuehn R, Tosun C, Caridi J, Keledjian K, Bochicchio G, Scalea T, Gerzanich V, Simard JM. Novel model of frontal impact closed head injury in the rat. J Neurotrauma. 2009;26(12):2233-43.
39. Czeiter E, Pal J, Kovesdi E, Bukovics P, Luckl J, Doczi T, Buki A. Traumatic Axonal Injury in the Spinal Cord Evoked by Traumatic Brain Injury. Journal of Neurotrauma. 2008;25(3):205-13.
40. Guo Y, Saunders T, Su H, Kim H, Akkoc D, Saloner DA, Hetts SW, Hess C, Lawton MT, Bollen AW. Silent intralesional microhemorrhage as a risk factor for brain arteriovenous malformation rupture. Stroke. 2012;43(5):1240.
41. Schreiber S, Bueche CZ, Garz C, Kropf S, Angenstein F, Goldschmidt J, Neumann J, Heinze HJ, Goertler M, Reymann KG. The pathologic cascade of cerebrovascular lesions in SHRSP: is erythrocyte accumulation an early phase? Journal of Cerebral Blood Flow & Metabolism Official Journal of the International Society of Cerebral Blood Flow & Metabolism. 2012;32(2):278-90.
42. Harrison EB, Emanuel K, Lamberty BG, Morsey BM, Li M, Kelso ML, Yelamanchili SV, Fox HS. Induction of miR-155 after Brain Injury Promotes Type 1 Interferon and has a Neuroprotective Effect. Frontiers in Molecular Neuroscience. 2017;10.
43. Li L, Chopp M, Ding G, Qu C, Nejad-Davarani SP, Davoodi-Bojd E, Li Q, Mahmood A, Jiang Q. Diffusion-derived MRI Measures of Longitudinal Microstructural Remodeling Induced by Marrow Stromal Cell Therapy after TBI. Journal of Neurotrauma. 2016;34(1).
44. Glushakova OY, Johnson D, Hayes RL. Delayed increases in microvascular pathology after experimental traumatic brain injury are associated with prolonged inflammation, blood-brain barrier disruption, and progressive white matter damage. Journal of Neurotrauma. 2014;31(13):1180.
45. MA F, PF S, KM B, SJ M, WR S, E S. Mouse closed head injury model induced by a weight-drop device. Nature protocols. 2009;4(9):1328-37.
46. Stahel PF, Flierl MA, Morgan BP, Persigehl I, Stoll C, Conrad C, Touban BM, Smith WR, Beauchamp K, Schmidt OI. Absence of the complement regulatory molecule CD59a leads to exacerbated neuropathology after traumatic brain injury in mice. Journal of Neuroinflammation. 2009;6(1):1-11.
47. Baguley IJ, Nott MT, Slewa-Younan S. Long-term mortality trends in functionally-dependent adults following severe traumatic-brain injury. Brain Injury. 2008;22(12):919-25.
48. Baguley IJ, Nott MT, Howle AA, Simpson GK, Browne S, King AC, Cotter RE, Hodgkinson A. Late mortality after severe traumatic brain injury in New South Wales: a multicentre study. Medical Journal of Australia. 2012;196(1):40-5.
49. Bigler ED, Bazarian JJ. Diffusion tensor imaging: a biomarker for mild traumatic brain injury? Neurology. 2010;74(8):626.
50. Kou Z, Wu Z, Tong KA, Holshouser B, Benson RR, Hu J, Haacke EM. The role of advanced MR imaging findings as biomarkers of traumatic brain injury. Journal of Head Trauma Rehabilitation. 2010;25(4):267.
51. Smith DH, Nonaka M, Miller R, Leoni M, Chen XH, Alsop D, Meaney DF. Immediate coma following inertial brain injury dependent on axonal damage in the brainstem. Journal of Neurosurgery.

2000;93(2):315.

52. Tomaiuolo F, Carlesimo G, Di P, Petrides M, Fera F, Bonanni R, Formisano R, Pasqualetti P, Caltagirone. Gross morphology and morphometric sequelae in the hippocampus, fornix, and corpus callosum of patients with severe non-missile traumatic brain injury without macroscopically detectable lesions: a T1 weighted MRI study. Journal of Neurology Neurosurgery & Psychiatry. 2004;75(9):1314.
53. Delanowood L, Bangen KJ, Sorg SF, Clark AL, Schiehser DM, Luc N, Bondi MW, Werhane M, Kim RT, Bigler ED. Brainstem white matter integrity is related to loss of consciousness and postconcussive symptomatology in veterans with chronic mild to moderate traumatic brain injury. Brain Imaging & Behavior. 2015;9(3):500.
54. Browne KD, Chen XH, Meaney DF, Smith DH. Mild traumatic brain injury and diffuse axonal injury in swine. Journal of Neurotrauma. 2011;28(9):1747.
55. Adelson PD, Jenkins LW, Hamilton RL, Robichaud P, Tran MP, Kochanek PM. Histopathologic response of the immature rat to diffuse traumatic brain injury. Journal of Neurotrauma. 2001;18(10):967.
56. Raghupathi R, Margulies SS. Traumatic axonal injury after closed head injury in the neonatal pig. Journal of Neurotrauma. 2002;19(7):843-53.
57. Flygt J, Djupsjö A, Lenne F, Marklund N. Myelin loss and oligodendrocyte pathology in white matter tracts following traumatic brain injury in the rat. European Journal of Neuroscience. 2013;38(1):2153-65.
58. Davidsson J, Risling M. A New Model to Produce Sagittal Plane Rotational Induced Diffuse Axonal Injuries. Frontiers in Neurology. 2011;2:41.
59. Hellewell SC, Yan EB, Agyapomaa DA, Bye N, Morganti-Kossmann MC. Post-traumatic hypoxia exacerbates brain tissue damage: analysis of axonal injury and glial responses. Journal of Neurotrauma. 2010;27(11):1997-2010.
60. Wang HY, Liu CB, Wu HW, Kuo JS. Direct profiling of phospholipids and lysophospholipids in rat brain sections after ischemic stroke. Rapid Communications in Mass Spectrometry Rcm. 2010;24(14):2057-64.
61. Liu MC, Akinyi L, Scharf D, Mo J, Larner SF, Muller U, Oli MW, Zheng W, Kobeissy F, Papa L. Ubiquitin C-terminal hydrolase-L1 as a biomarker for ischemic and traumatic brain injury in rats. European Journal of Neuroscience. 2010;31(4):722-32.
62. Bogoslovsky T, Wilson D, Chen Y, Hanlon D, Gill J, Jeromin A, Song L, Moore C, Gong Y, Kenney K. Increases of Plasma Levels of Glial Fibrillary Acidic Protein, Tau and Amyloid Beta 42 up to 90 Days Following Traumatic Brain Injury. Journal of Neurotrauma. 2016;34(1):66.
63. Yang S, Sun R, Zhou Z, Zhou J, Liang J, Mu H. Expression of Amyloid-β Protein and Amyloid-β Precursor Protein After Primary Brain-Stem Injury in Rats. American Journal of Forensic Medicine & Pathology. 2014;35(3):201-5.

64. Sundman MH, Hall EE, Chen NK. Examining the relationship between head trauma and neurodegenerative disease: A review of epidemiology, pathology and neuroimaging techniques. Journal of Alzheimers Disease & Parkinsonism. 2014;4(1).
65. EG, Morenogonzalez I, Soto C. Amyloid-beta and tau pathology following repetitive mild traumatic brain injury. Biochemical & Biophysical Research Communications. 2016;483(4):1137.
66. Taylor JM, Kelley B, Gregory EJ, Berman NEJ. Neuroglobin overexpression improves sensorimotor outcomes in a mouse model of traumatic brain injury. Neuroscience Letters. 2014;577:125-9.
67. Anderson J, Sandhir R, Hamilton ES, Berman NE. Impaired expression of neuroprotective molecules in the HIF-1alpha pathway following traumatic brain injury in aged mice. Journal of Neurotrauma. 2009;26(9):1557.
68. Chuang PY, Conley YP, Poloyac SM, Okonkwo DO, Ren D, Sherwood PR, Hravnak M, Alexander SA. Neuroglobin genetic polymorphisms and their relationship to functional outcomes after traumatic brain injury. Journal of Neurotrauma. 2010;27(6):999-1006.
69. Di PV, Lazzarino G, Amorini AM, Tavazzi B, D'Urso S, Longo S, Vagnozzi R, Signoretti S, Clementi E, Giardina B. Neuroglobin expression and oxidant/antioxidant balance after graded traumatic brain injury in the rat. Free Radical Biology & Medicine. 2014;69(4):258-64.
70. X, Li M, Shang A, Hu Y, Yang X, Ye L, Bian S, Wang Z, Zhou D. Neuroglobin expression in rats after traumatic brain injury. Neural regeneration research. 2012;7(25):1960.

Figures

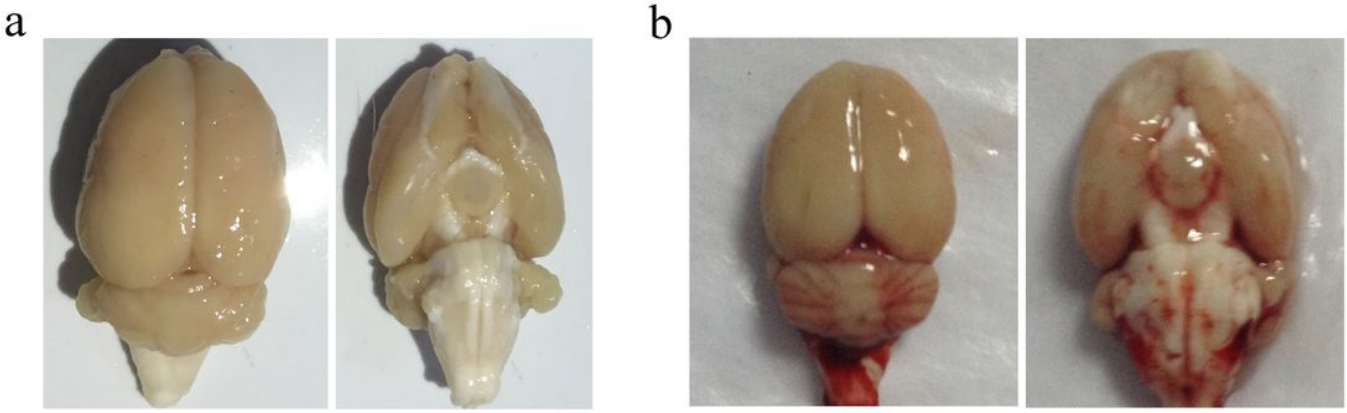

Figure 1

The brainstem gross observation of TBI group was obvious compared with controls. The control group had no abnormity (1a). Swelling brain tissue, dilatating and congesting vessels, prominent subarachnoid hemorrhage located at the base of brain and BS could be observed in the TBI group (1b).

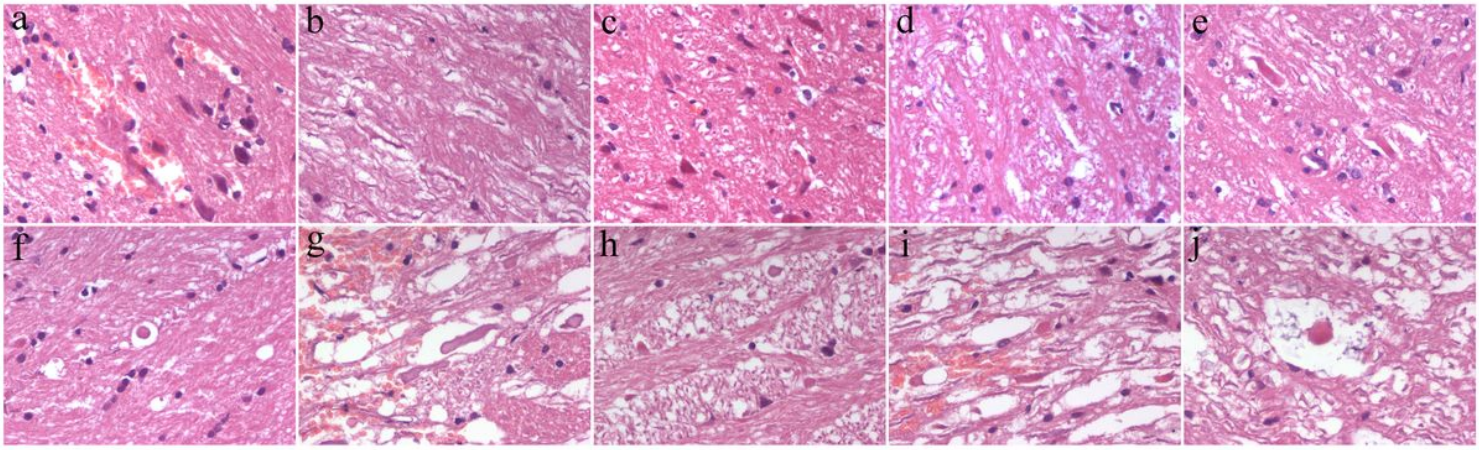

Figure 2

TBI-induced neuronal death and axonal demyelination. Contusion, interstitial edema, degenerative and necrotic neurons could be seen in the injured groups (2a – 2c). At 1h post-injury, the axons were irregular edema and wavy changes (2d). Mild circuity and inflated terminal of the axons appeared and the retraction balls (RBs) started to form at 3h group (2e). The number and range of damage axons gradually increased from 6h to 24h (2f - 2h). Among these time points, the number of RBs were significantly risen in 24h group. The region of swelling axons and the number of RBs slightly declined from 48h to 72h (2i-2j). The sections (4 μm thickness) through the brainstem were stained with H & E staining for microscopic analysis to determine the neuronal damage and axonal demyelination (n = 10 in each group, Scale bar = 2.5 μm).

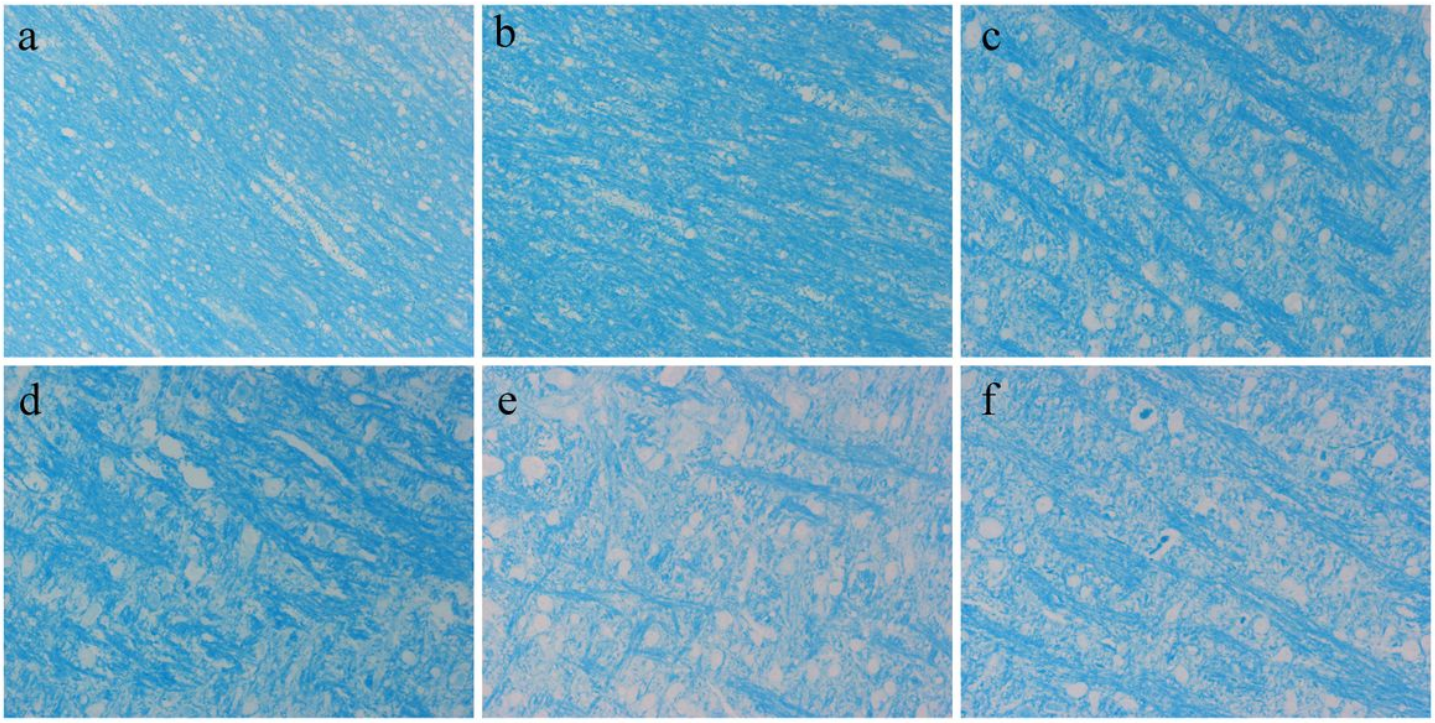

Figure 3

LFB staining showed that nerve myelin was neatly arranged in the sham group (3a). Swollen, layered, separated and disintegrated nerve myelin appeared at 1h (3b). The range of edema and disintegration were further enlarged and the number of clumps caused by the aggregative myelin were increased from 3h - 6h (3c). As for the injured 12h group, the number of clumps resulted from myelin disintegration and fragmentation was further enlarged (3d). The diffuse distribution of myelin was disorganized and significant vacuolar degeneration at 24h point (3e). The number of myelin fragments was reduced from 48h – 72h after injury (3f). The sections (4 μm thickness) through the brainstem were stained with luxol fast blue (LFB) for microscopic analysis to determine the axonal demyelination (n = 10 in each group, Scale bar = 5 μm).

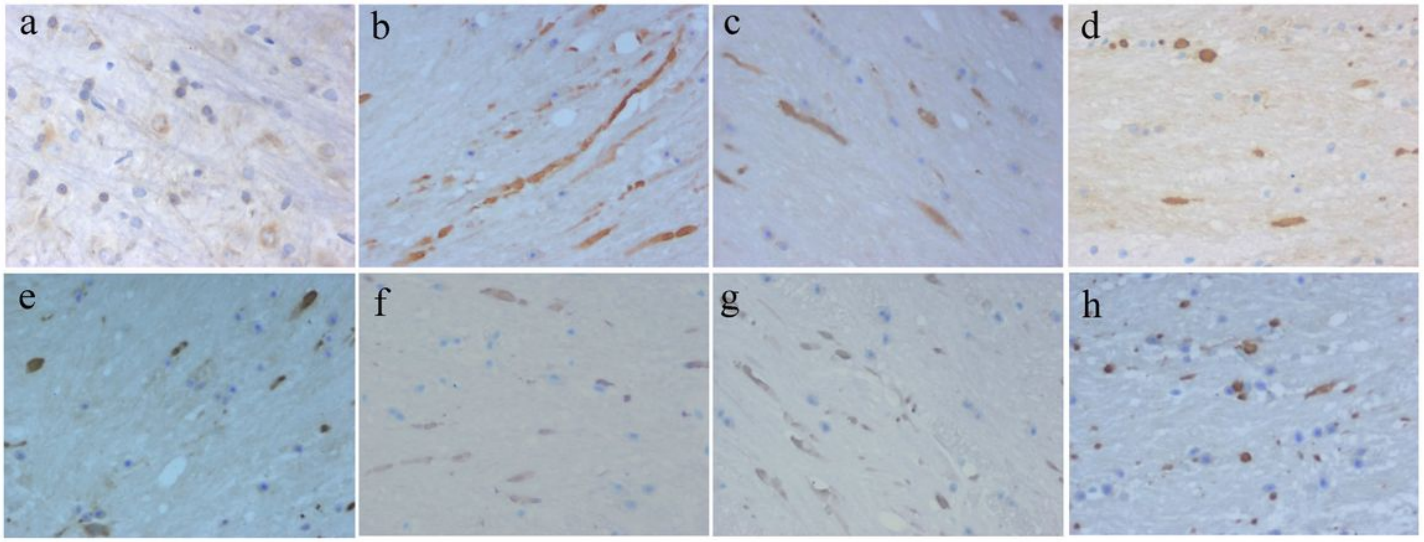

Figure 4

The BS sections were stained with the anti-β-APP antibody for further verification of TBI. At the control group, the IHC staining of β-APP was weakly positive (4a). β-APP positive axons were slightly circuitous, swelling and beaded change since 1h post-TBI (4b). A few RBs formed at 3h group (4c), the number of immunopositivity RBs increased and became more obvious from 3h - 6h (4d). The positive axons were obvious, and the number and range of RBs were further expanded after 12h post-TBI (4e). Typical RBs were gradually increased from 24h - 72h and reaching the maximum at 72h (4f - 4h) (n = 10 in each group, Scale bar = 2.5 μm).

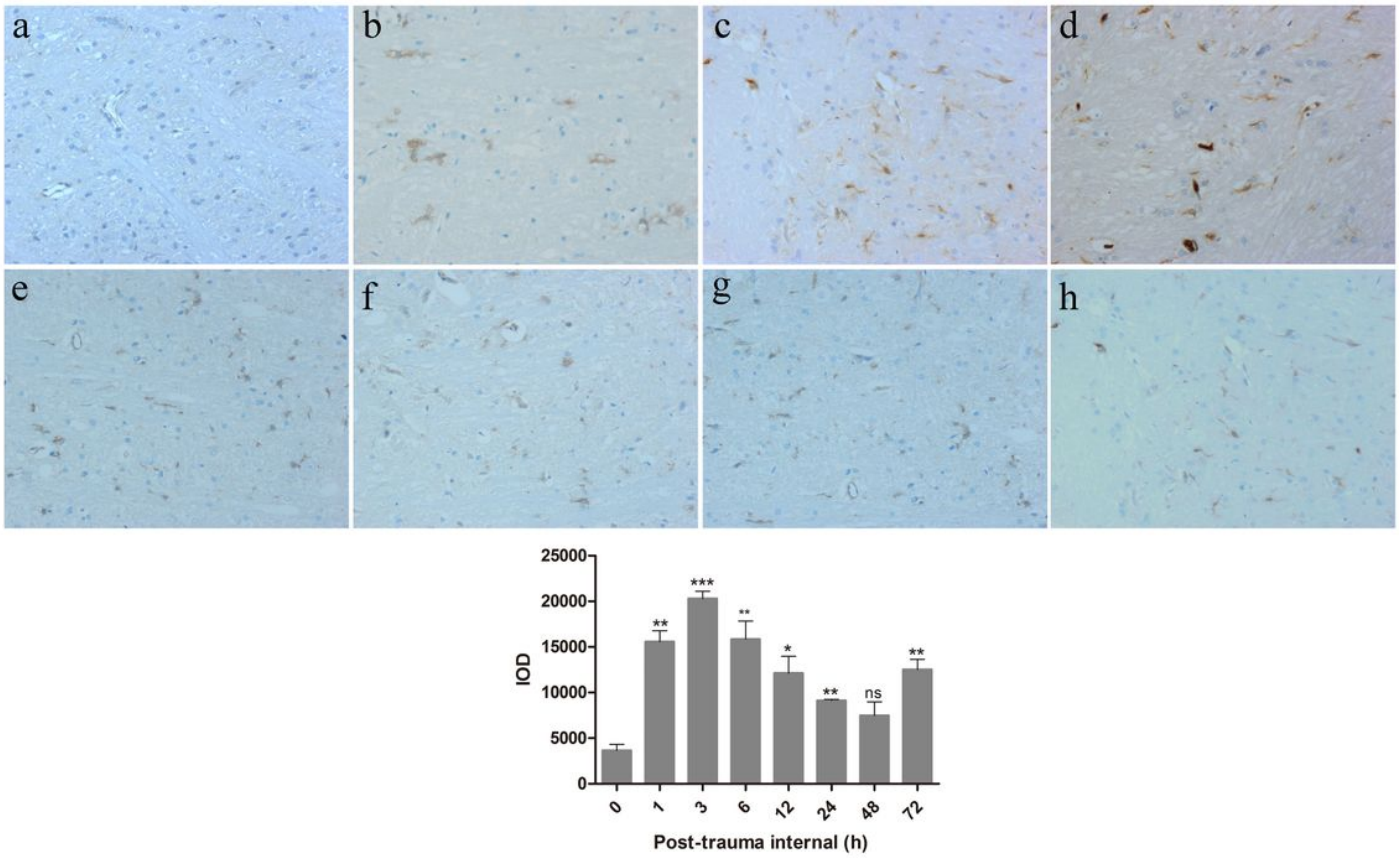

Figure 5

The IHC analysis of BS after traumatic brain injury (TBI). The top half of the chart show Aβ expression during TBI; Times are indicated in numerals and represent hours after injury. The positive cytoplasm and small blood vessels of the BS were enlarged at all points after TBI. The bottom half of the chart reveal quantification of Aβ protein expression. Semiquantitative densitometry in conjunction with AlphaEase software was used for the quantification, and the data are expressed as mean ± S.E.M. Representative results of at least three experiments are shown. Scale bar = 5 μm, ns, no significance. (n = 10 in each group, *p□0.05, ** P < 0.01 and *** P < 0.0001).

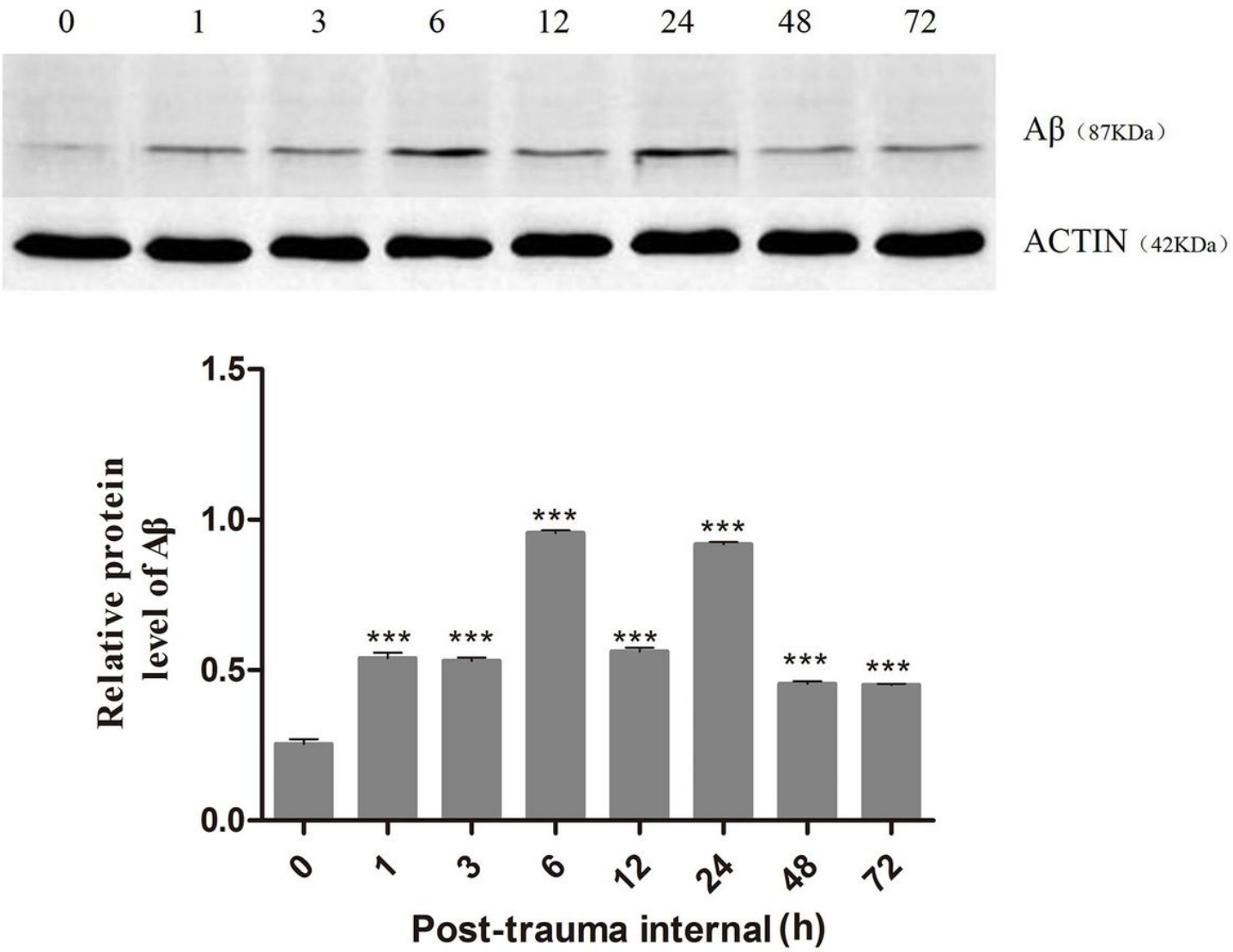

Figure 6

Western blot analysis of Aβ levels in BS following TBI for various times. β-actin was used as a loading control. The analysis revealed that Aβ expression of all experimental groups were higher than the control group, the 6h and 24h groups were extremely significant difference compared with the control group. Data are expressed as mean ± S.E.M. Representative results of three experiments are shown (n = 10 in each group, *** $P < 0.0001$).

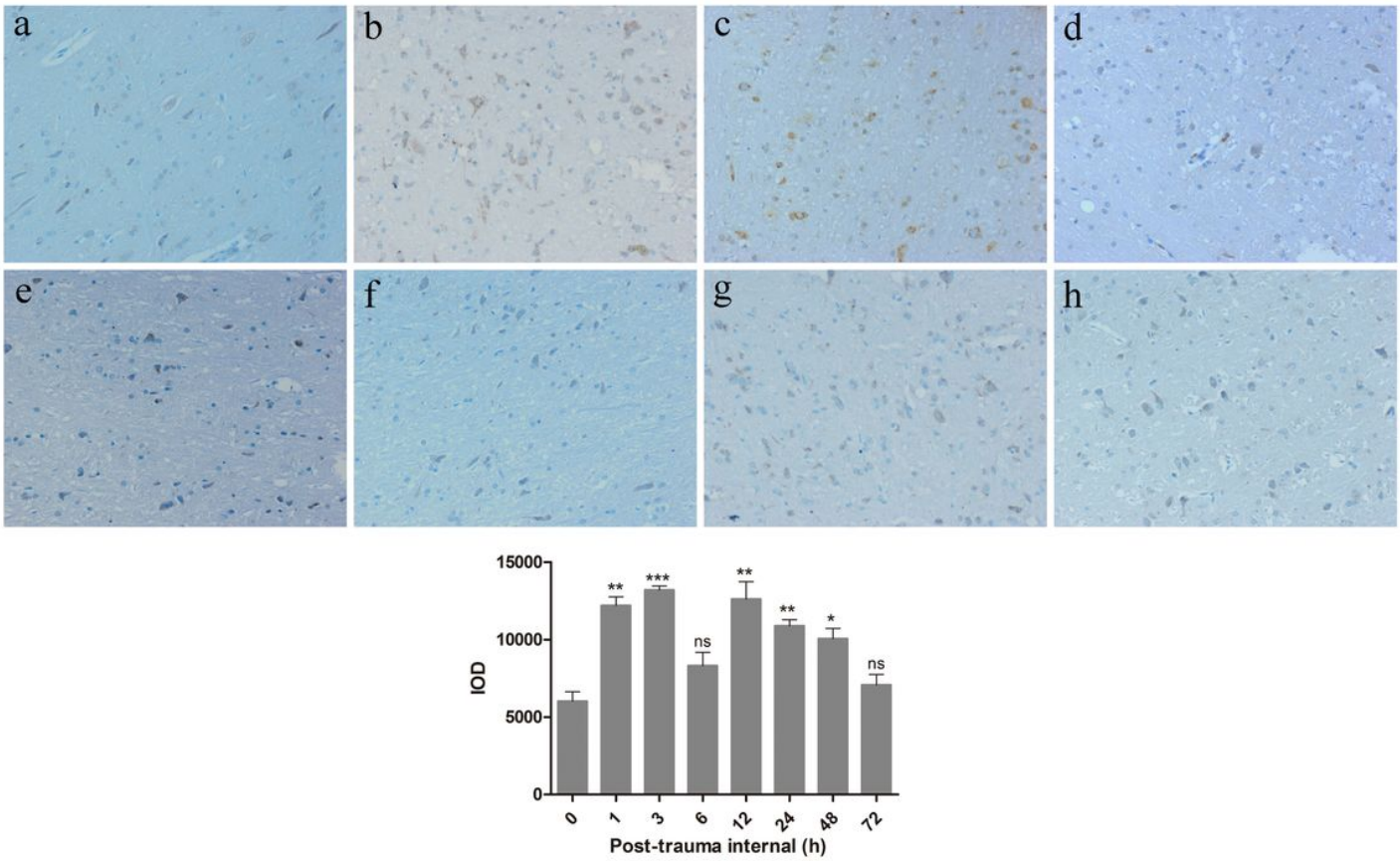

Figure 7

Expression of Neuroglobin in rat brainstem after traumatic brain injury (TBI). Immunohistochemical results of the rat brainstem 0 (control, no injury), 1, 3, 6, 12, 24, 48 and 72 hours after TBI. Increased NGB intensity in brainstems was observed as early as 1 hour after the injury and became substantially evident 1–48 hours. Graphical representation of NGB positive staining using immunohistochemical intensity. Data are expressed as mean ± S.E.M. Representative results of three experiments are shown Scale bar = 5 μm, ns, no significance. (n = 10 in each group, *p□0.05, ** P < 0.01 and *** P < 0.0001).

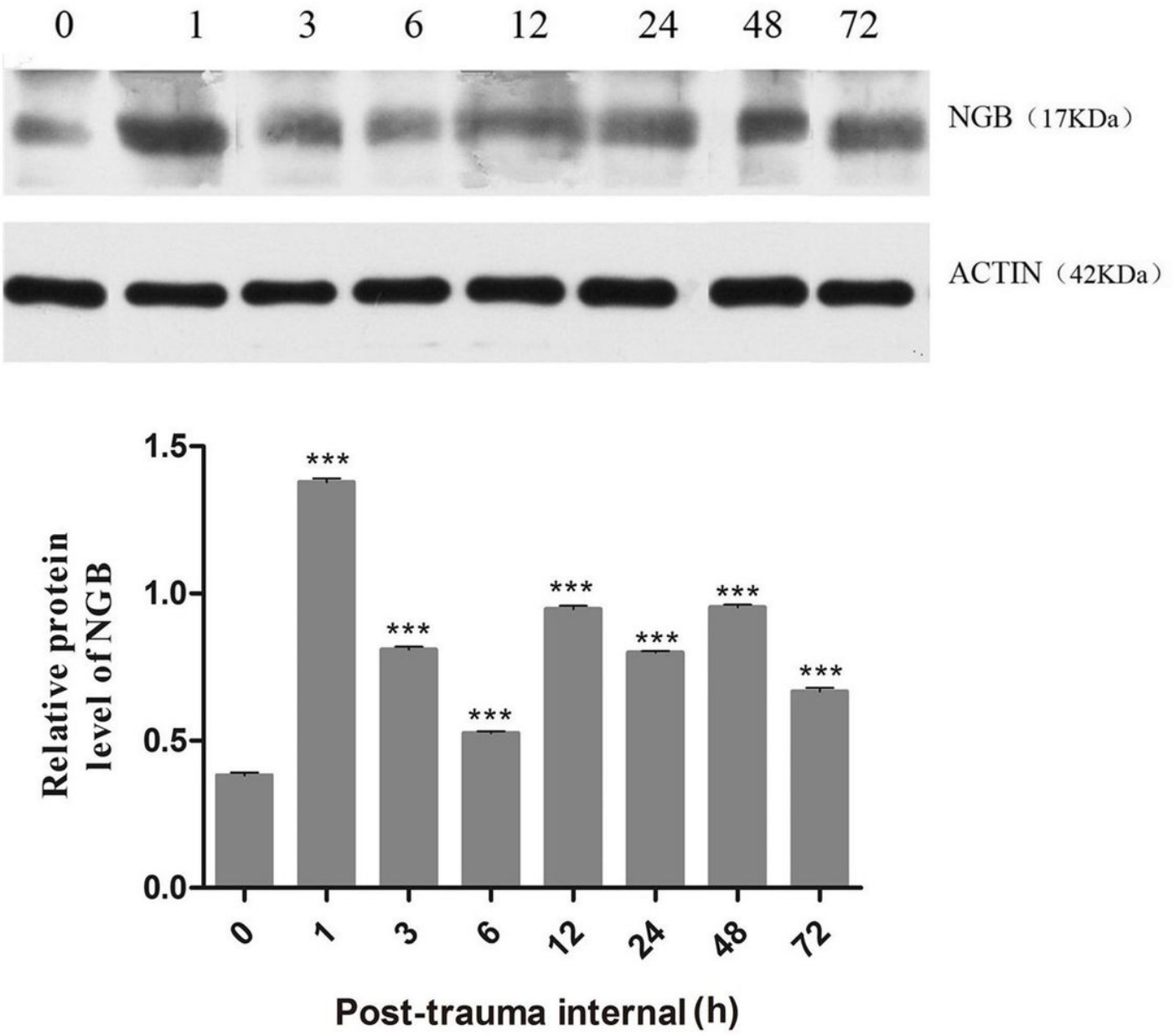

Figure 8

Western blot analysis of NGB in the brainstem for 0 (control), 1, 3, 6, 12, 24, 48 and 72 hours after traumatic brain injury. β-actin was used as a loading control. The analysis revealed that NGB expression of all experimental groups were higher than the control group, the 1h group was extremely significant difference compared with the other group. Data are expressed as mean ± S.E.M. Representative results of three experiments are shown (n = 10 in each group, *** $P < 0.0001$).

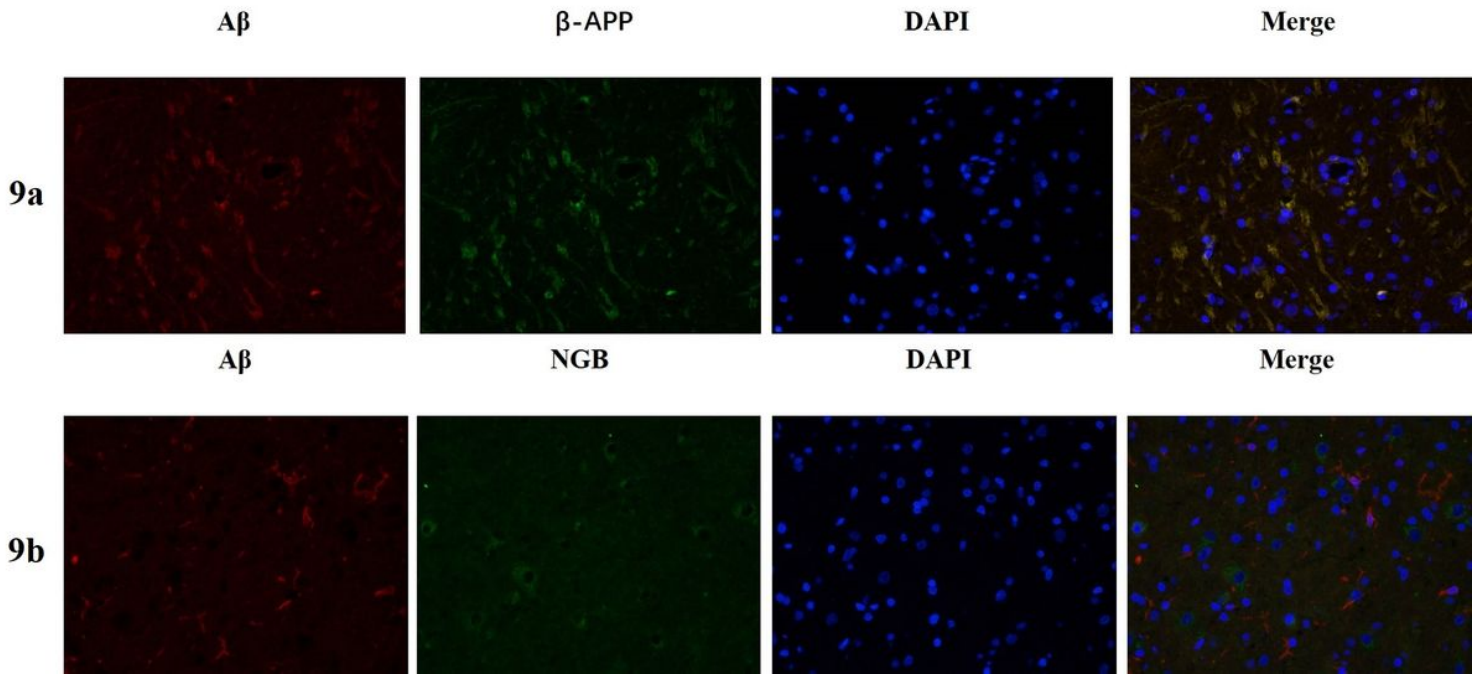

Figure 9

Immunofluorescent analysis of the accumulation of Aβ (red), β – APP and NGB (green) by confocal microscopy. Nuclei were stained with DAPI (blue). Many of the Aβ positive sites showed co-localization with β - APP. The result suggested that β - APP and Aβ were distributed in neurons and axons (9a). Similar patterns of punctate labeling, but found that areas of more concentrated NGB deposition were localized within Aβ -positive neurons. The results supported that Aβ and NGB co-localization in the neurons of BS (9b) (Scale bars: 2.5 μm).